

Scaling corrections in driven critical dynamics: Application to the two-dimensional dimerized quantum Heisenberg model

Jing-Wen Liu(刘静雯), Shuai Yin(阴帅), and Yu-Rong Shu(舒玉蓉)
Citation: Chin. Phys. B, 2025, 34 (**5**): 057502. DOI: 10.1088/1674-1056/adc672
http://cpb.iphy.ac.cn; http://iopscience.iop.org/cpb

What follows is a list of articles you may be interested in

Analysis of pseudo-random number generators in QMC-SSE method

Dong-Xu Liu(刘东旭), Wei Xu(徐维), and Xue-Feng Zhang(张学锋)
Chin. Phys. B, 2024, 33 (**3**): 037509. DOI: 10.1088/1674-1056/ad1e69

Emergent O(4) symmetry at the phase transition from plaquette-singlet to antiferromagnetic order in quasi-two-dimensional quantum magnets

Guangyu Sun(孙光宇), Nvsen Ma(马女森), Bowen Zhao(赵博文), Anders W. Sandvik, and Zi Yang Meng(孟子杨)
Chin. Phys. B, 2021, 30 (**6**): 067505. DOI: 10.1088/1674-1056/abf3b8

Magnetic excitations of diagonally coupled checkerboards

Tingting Yan(颜婷婷), Shangjian Jin(金尚健), Zijian Xiong(熊梓健), Jun Li(李军), and Dao-Xin Yao(姚道新)
Chin. Phys. B, 2021, 30 (**10**): 107505. DOI: 10.1088/1674-1056/ac1b94

Tunable deconfined quantum criticality and interplay of different valence-bond solid phases

Bowen Zhao(赵博文), Jun Takahashi, Anders W. Sandvik
Chin. Phys. B, 2020, 29 (**5**): 057506. DOI: 10.1088/1674-1056/ab889b

Role of the spin anisotropy of the interchain interaction in weakly coupled antiferromagnetic Heisenberg chains

Yuchen Fan(樊宇辰), Rong Yu(俞榕)
Chin. Phys. B, 2020, 29 (**5**): 057505. DOI: 10.1088/1674-1056/ab820b

---

RAPID COMMUNICATION

Scaling corrections in driven critical dynamics: Application to the two-dimensional dimerized quantum Heisenberg model

Jing-Wen Liu(刘静雯)[1], Shuai Yin(阴帅)[2], and Yu-Rong Shu(舒玉蓉)[1,†]

[1] *School of Physics, Guangzhou University, Guangzhou* 510275, *China*

[2] *Guangdong Provincial Key Laboratory of Magnetoelectric Physics and Devices, School of Physics, Sun Yat-Sen University, Guangzhou* 510275, *China*

(Received 13 February 2025; revised manuscript received 27 March 2025; accepted manuscript online 28 March 2025)

Driven critical dynamics in quantum phase transitions holds significant theoretical importance, and also has practical applications in fast-developing quantum devices. While scaling corrections have been shown to play important roles in fully characterizing equilibrium quantum criticality, their impact on nonequilibrium critical dynamics has not been extensively explored. In this work, we investigate the driven critical dynamics in a two-dimensional quantum Heisenberg model. We find that in this model the scaling corrections arising from both finite system size and finite driving rate must be incorporated into the finite-time scaling form in order to properly describe the nonequilibrium scaling behaviors. In addition, improved scaling relations are obtained from the expansion of the full scaling form. We numerically verify these scaling forms and improved scaling relations for different starting states using the nonequilibrium quantum Monte Carlo algorithm.

Keywords: driven critical dynamics, scaling correction, quantum Monte Carlo

PACS: 75.40.Gb, 05.70.Jk, 64.60.Ht, 75.40.Mg

DOI: 10.1088/1674-1056/adc672 **CSTR:** 32038.14.CPB.adc672

1. Introduction

Developing universal scaling theories to characterize the nonequilibrium dynamics of phase transitions is of broad significance across diverse fields, including statistical mechanics, condensed matter physics, and rapidly advancing quantum computing platforms.[1–5] One of the simplest approaches to realize the nonequilibrium critical dynamics involves driving a system by tuning a relevant parameter across the critical point. The Kibble–Zurek mechanism (KZM) provides a general framework for understanding this kind of driven dynamics. It predicts the emergence of an impulse region around the critical point, where the system cannot evolve adiabatically under the external driving due to critical slowing down, leading to the formation of topological defects after the quench.[6,7] Furthermore, the KZM establishes that the velocity dependence of the density of these topological defects satisfies the scaling relation characterized by the equilibrium critical exponents, thereby bridging the gap between the equilibrium universality and the nonequilibrium critical dynamics.[6,7] The KZM has been verified in a wide range of systems, including both classical and quantum phase transitions.[8–17]

On the other hand, in analogy with the well-established equilibrium finite-size scaling (FSS), which shows that the system size L governs the critical properties when the equilibrium correlation length ξ_e (defined as $\xi_e \propto |g|^{-\nu}$ with g being the distance to the critical point and ν being the corresponding critical exponent) exceeds L, the finite-time scaling (FTS) was proposed as a temporal counterpart of FSS for driven critical dynamics.[18–20] By introducing a driving-induced time scale as $\zeta_d \propto R^{-z/r}$, in which R is the driving velocity with a critical dimension of r and z is the dynamic exponent, the FTS theory demonstrates that R dominates the dynamic scaling behaviors when ζ_d is smaller than the equilibrium correlation time scale $\zeta_e \propto \xi_e^z$.[18–20]

Comparing the FTS theory with the KZM, one finds that the FTS region dominated by R is just the impulse region of the KZM.[21,22] In addition, the FTS remarkably generalizes the KZM by providing a framework to understand the scaling behaviors of all macroscopic quantities throughout the entire driven process,[21,22] whereas the original KZM primarily focuses on the scaling of topological defects after the quench.[2,3,6,7] Moreover, the FTS can accommodate different types of driven dynamics for different driving forces, such as changing the symmetry-breaking field,[18] lowering the temperature near the quantum critical point,[23] and others. Recently, it has been demonstrated that the full scaling form of the FTS remains applicable in driven dynamics even beyond the adiabatic-impulse prerequisite of the KZM.[24–26] Similar full scaling forms have also been explored in other contexts,[27–30] and their validity has been confirmed in experimental studies.[31–34]

Despite many successes, scaling theories that focus only on relevant scaling variables have limitations in capturing universal properties in practical applications. In real systems,

†Corresponding author. E-mail: yrshu@gzhu.edu.cn

© 2025 Chinese Physical Society and IOP Publishing Ltd. All rights, including for text and data mining, AI training, and similar technologies, are reserved.

the coupling term can deviate from its fixed point, and irrelevant perturbations may also present. As a result, incorporating scaling corrections that account for these irrelevant perturbations is essential to further improve the scaling theories.[35,36] While such corrections are commonly considered in equilibrium FSS,[36] explorations of their roles in nonequilibrium critical dynamics are relatively rare, with only some formal discussion in Ref. [20]. Given the importance of driven critical dynamics, investigating scaling corrections in nonequilibrium FTS is highly desired.

In this paper, we explore the driven critical dynamics in a two-dimensional (2D) dimerized Heisenberg model with $S = 1/2$. Previous studies have shown that this model harbors a quantum phase transition (QPT) between the Néel antiferromagnetic (AFM) and quantum paramagnetic (PM) phases, with the transition belonging to the $(2+1)$D Heisenberg universality class.[36–56] We find that in order to appropriately describe the critical dynamics in this model, it is necessary to include scaling corrections from both finite system size and finite driving rate within the FTS form. Specifically, for small driving rates, scaling corrections are mainly influenced by the finite system size, while for large driving rates, the corrections are mainly from the driving rate. Improved scaling relations are obtained from the expansion of the full scaling form. We numerically verify the scaling form and the improved scaling relations for different starting states using the nonequilibrium quantum Monte Carlo (NEQMC) algorithm.[36] Our work not only reveals the driven critical dynamics in the Heisenberg universality class, but also provides a systematic scaling analysis of the scaling corrections in FTS, which can be generalized to other systems.

The paper is structured as follows. We first introduce the spin model and the numerical method in Section 2, then outline the FTS framework with scaling corrections in Section 3, and present numerical results on the critical dynamics of the Binder ratio and the order parameter from different starting states in Section 4. Finally, a summary is given in Section 5.

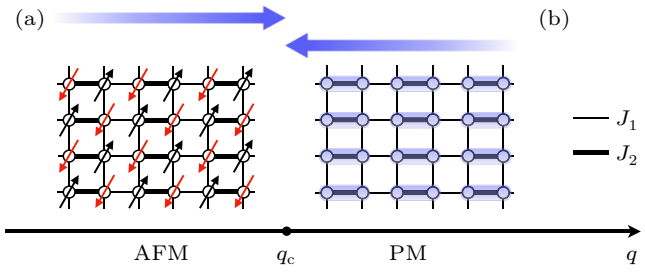


Fig. 1. Sketch of the phase diagram and the driven critical dynamics with different initial states. J_1 and J_2 are the antiferromagnetic couplings on nearest-neighbor bonds $\langle ij\rangle$ (thin) and $\langle ij\rangle'$ (thick), respectively. The initial states are prepared as the Néel AFM state and the columnar dimerized PM state with the colored bonds representing manual columnar dimerization. The arrows indicated by (a) and (b) represent the driving starting from the AFM state and PM state, respectively.

2. Model and method

The Hamiltonian of the 2D dimerized Heisenberg model is given by[37–41]

$$H = J_1 \sum_{\langle ij\rangle} \boldsymbol{S}_i \cdot \boldsymbol{S}_j + J_2 \sum_{\langle ij\rangle'} \boldsymbol{S}_i \cdot \boldsymbol{S}_j, \tag{1}$$

in which $\boldsymbol{S}_i = (1/2)(\sigma_x, \sigma_y, \sigma_z)$ denotes the spin-1/2 operator at site i, and J_1 and J_2 represent the antiferromagnetic couplings on bonds $\langle ij\rangle$ and $\langle ij\rangle'$, as denoted by the thin and thick bonds in Fig. 1, respectively. Note that here J_1 and J_2 couplings are defined on different sets of nearest-neighbor bonds and should not be confused with the case where J_2 typically represents the next-nearest-neighbor interactions.

The QPT in this model has attracted significant attention,[36–56] due to its relevance as a prototypical example of a system where the ordered phase spontaneously breaks the continuous symmetry, and also its close relation to strongly-correlated materials such as the cuprate superconductors.[47,57–59] By tuning the ratio $q \equiv J_2/J_1$, a QPT occurs at $q_c = 1.90951(5)$,[52] separating the Néel AFM order[36,52] for $q < q_c$ from the paramagnetic (PM) phase for $q > q_c$. The order parameter characterizing the transition is $\boldsymbol{M} \equiv (1/L^2)\sum_r (-1)^{r_x+r_y}\boldsymbol{S}_r$, where r_x and r_y are the coordinates of lattice sites in the x and y directions, respectively. The criticality near this QPT is well described by the Heisenberg $O(3)$ universality class,[37,41,47] as verified with scrutiny by numerical simulations using efficient QMC methods.[36]

The foundation of the FTS theory involves preparing a starting state, which is the ground state for a parameter q_0 far from the critical point. The system is then driven by a linearly varying q across the critical point with a finite driving rate R.[18,19,21–23] However, directly simulating the real-time dynamics in 2D systems remains beyond the reach of current numerical methods. Fortunately, it has been shown that the driven critical dynamics in the imaginary-time direction shares the same scaling forms and critical exponents with that in the real-time direction, with differences only in the detailed scaling functions.[28] The reason is that for both real- and imaginary-time cases, the only parameter that characterizes the deviation from equilibrium is the driving rate R. As such, R serves as a natural characteristic quantity for describing the nonequilibrium dynamic scaling behaviors in both real- and imaginary-time directions. Scaling analyses also indicate that the driving rate shares the same critical dimension in both real- and imaginary-time driven dynamics. This allows us to probe the universal scaling properties in the real-time direction through the imaginary-time dynamics, which can be accessed using the QMC method for sign-problem-free models.[24–26,60]

In this work, we use the NEQMC method to realize the imaginary-time driven dynamics. To avoid confusion with real time t, we denote the imaginary evolution time by τ.

Since the Hamiltonian is time-dependent, the evolution of the state obeys the analogue of Schrödinger dynamics, such that $|\psi(\tau)\rangle = U(\tau)|\psi(\tau_0)\rangle$, where $|\psi(\tau_0)\rangle$ is the starting state at $\tau_0 = 0$ and $U(\tau) = T_\tau \exp\left[-\int_{\tau_0}^{\tau} \mathrm{d}\tau' H(\tau')\right]$ is the Euclidean time evolution operator, with T_τ ensuring time ordering. As in the standard time-independent projector QMC method, the evolution operator $U(\tau)$ is expanded in a power series and applied to the starting state $|\psi(\tau_0)\rangle$. After splitting the Hamiltonian into bond operators, inserting additional unit operators and their corresponding time integrals, the power series can be truncated and importance samplings of the normalization $Z = \langle\psi(\tau)|\psi(\tau)\rangle$ are carried out in a proper basis, such as the spin-z basis. A full Monte Carlo sweep of the importance sampling procedure involves updates of the operator sequence, the basis state (which are mostly the same as those in the standard projector QMC method) and additionally, the time sequence needed in sampling the time integrals. Measurements are performed in the middle of the projection $A(\tau) = \langle\psi(\tau)|A|\psi(\tau)\rangle/Z$. We refer the technical details of the NEQMC method to the literature.[28,60–62] For the model studied here, we set $J_1 = 1$ and therefore $q = J_2$ varies following $q(\tau) = q_0 \pm R\tau$. For a driving from q_0 to q_c with a given driving rate, the total simulation time is $\tau_a = |q_c - q_0|/R$, and the total computation effort scales as $L^d\tau_a$.

3. General scaling theory

We begin with the general FTS form of a quantity $\mathcal{Q}$.[18–23] In the following, we focus on the case for drivings terminated at the critical point $q = q_c$. Including the scaling corrections, the scaling form is given by

$$\mathcal{Q}(R,L) = L^{\kappa} f_Q(RL^r, L^{-\omega}), \tag{2}$$

in which κ is the scaling dimension of $\mathcal{Q}$, and ω is the correction exponent. For the $(2+1)$D Heisenberg universality class, $\omega = 0.78$, which is analytically obtained in Ref. [63] and numerically verified in Ref. [52]. In the scaling function f_Q, the first term arises from the fact that $R^{-1/r}$ (with $r = z + 1/\nu$) has the scaling dimension of L,[18–23] the second term corresponds to the scaling correction comes from finite system size. Moreover, f_Q depends on the driving directions.

One can expand the scaling function on the scaling correction term to the leading order as

$$\mathcal{Q}(R,L) = L^{\kappa}\left[1 + L^{-\omega} g_Q(RL^r)\right] f_{Q0}(RL^r), \tag{3}$$

in which f_{Q0} is another scaling function. $g_Q(RL^r)$ tends to its equilibrium value for small R, while $g_Q(RL^r)$ should satisfy $g_Q(RL^r) \propto (RL^r)^{\omega/r}$ for large R, giving rise to the FTS correction term, characterized by $R^{\omega/r}$.[20] Accordingly, for general RL^r, as a first-order approximation, one can assume that $g_Q(RL^r)$ is a linear combination of the forms for small and large RL^r. Accordingly, $L^{-\omega} g_Q(RL^r)$ can be approximated as $L^{-\omega} g_Q(RL^r) \approx b_Q L^{-\omega} + a'_Q R^{\omega/r}$, in which b_Q is the coefficient of finite-size correction and a'_Q is another coefficient for $R^{\omega/r}$.

In order to separate the equilibrium finite size corrections, we can further incorporate term $a'_Q R^{\omega/r}$ into the scaling function. In this way, we can approximate the scaling form as

$$\mathcal{Q}(R,L) = L^{\kappa}(1 + b_Q L^{-\omega}) f_{Q1}[RL^r(1 + a_Q R^{\omega/r})], \tag{4}$$

in which a_Q is the coefficient of the finite-driving-rate correction.

Although deriving Eq. (4) from first principles is challenging, we can inspect its validity based on the following considerations. First, in the limit $R \to 0$, Eq. (4) reduces to the equilibrium scaling form with finite-size correction, given by $\mathcal{Q}(L) = L^{\kappa}(1 + b_Q L^{-\omega})$. Second, for large R, the argument in f_{Q1} captures the crossover to the FTS region governed by R, where the dominant scaling correction arises from the finite driving rate. In particular, the dimensionless variable RL^r should be multiplied by a factor $(1 + cR^{\omega/r})$ (c is a nonuniversal constant), in analogy to the scaling correction for dimensionless quantities in conventional FSS.[36,52] This justifies the form of the argument in f_{Q1}. In the following, we will verify the validity of Eq. (4) for different quantities in the driven critical dynamics of the 2D dimerized Heisenberg model, considering both the AFM and PM starting states, as illustrated in Fig. 1.

4. Numerical results

We first examine the dynamics of the dimensionless Binder cumulant U, defined as $U \equiv (5/2)[1 - \langle M^4\rangle/(3\langle M^2\rangle^2)]$.[36] According to Eq. (4), U should satisfy

$$U(R,L) = (1 + b_U L^{-\omega}) f_U[RL^r(1 + a_U R^{\omega/r})], \tag{5}$$

in which both f_U and a_U are dependent on the driving process.

For the driven dynamics starting from the AFM side, we set $J_2 = 1$, namely, $q_0 = 1$ and drive the system towards the critical point $q_c = 1.90951$[52] with different rate R. The dependence of U on R is shown in Fig. 2(a). After rescaling R as RL^r without applying scaling corrections, the rescaled curves collapse in the large-R region, but significant deviations remain in the small-R region, as shown in Fig. 2(b). It might seem that the finite-size correction is adequate to address the discrepancy. As shown in Fig. 2(c), when the finite-size correction $(1 + b_U L^{-\omega})$ is included, the collapse is indeed considerably improved in the small-R region, however, the rescaled curves instead deviate from each other in the large-R region. To rectify this issue, we further incorporate the finite-R scaling correction $(1 + a_U R^{\omega/r})$ according to Eq. (5). Here the value of b_U is fixed and a_U is adjustable. By performing data collapse, we find $a_U = -1.18(7)$, with the number in parentheses

representing one standard deviation, the rescaled curves collapse successfully in the entire scaling region, confirming the validity of Eq. (5), as shown in Fig. 2(d).

Similar analyses can be found in the driven dynamics from the PM starting state. In this case, the starting PM state is realized by setting $J_2 = 3.0$ and the system is driven towards the critical point $q_c = 1.90951$.[52] In Fig. 3(a) we show the dependence of U on R for different system size L. After rescaling the curves of U versus R without any corrections, significant deviations appear in the rescaled curves. To better visualize these deviations, we show the small-R and large-R regions separately in Figs. 3(b) and 3(c), respectively. Introducing the finite-size scaling correction $(1+b_U L^{-\omega})$ with $b_U = 1.22$ (the equilibrium coefficient[52,64]) successfully collapses the rescaled curves in the small-R region (see Fig. 3(d)), but hardly improves the collapse in the large-R region (see Fig. 3(e)). To remedy this, we include the finite-R scaling correction $(1+a_U R^{\omega/r})$ as given in Eq. (4), which primarily affects the scaling in the large-R region as it vanishes for $R \to 0$. We find in Fig. 3(f) that with $a_U = -0.35(3)$, the entire rescaled curves collapse well, confirming the validity of Eq. (5).

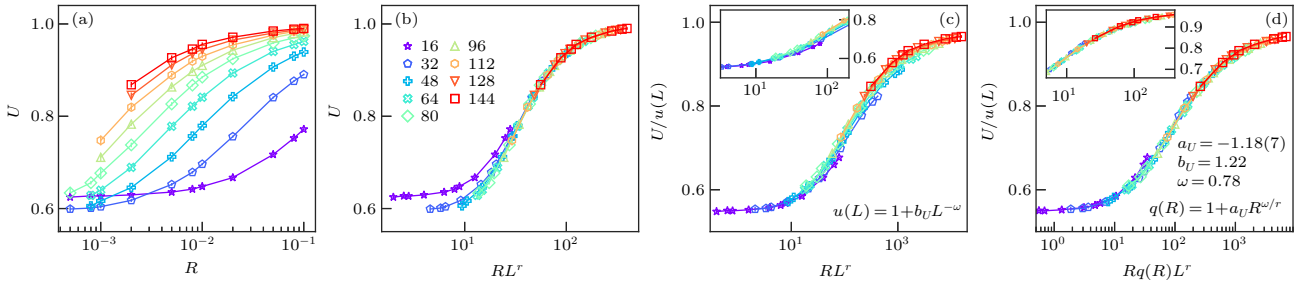


Fig. 2. (a) Dependence of the Binder cumulant U on the driving rate R starting from the AFM state with $q_0 = 1$. (b) When rescaling R as RL^r, significant deviations appear in the small-R region. (c) Including the finite-size correction, the deviations in the small-R region is remedied but the rescaled curves in the large-R region deviate. (d) Including both the finite-size and finite-R corrections, the rescaled curves collapse well in the entire scaling region. The correction power and coefficients are given in (d). Log scale is applied in the x-axis in all panels.

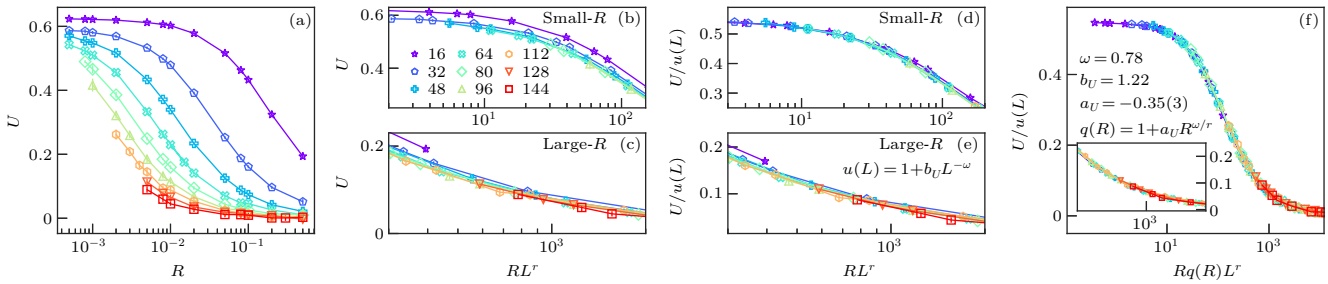


Fig. 3. (a) Dependence of the Binder cumulant U on the driving rate R starting from the PM state with $q_0 = 3$. (b) and (c) Zoom-in rescaled curves of U versus RL^r for the small-R and large-R regions, respectively. Clear deviations in the rescaled curves can be observed. (d) and (f) Rescaled curves with finite-size correction included for the small-R and large-R regions, respectively. The collapse in the small-R region is significantly improved but remains unsuccessful in the large-R region. (f) Including both the finite-size and finite-R corrections, the rescaled curves collapse well in the entire scaling region. The correction power and coefficients are given in panel (f). Log scale is applied in the x-axis in all panels.

Next we analyze the dynamics of the squared order parameter M^2. According to Eq. (4), M^2 should obey[18–23]

$$M^2(R,L) = L^{-2\beta/\nu}(1+b_M L^{-\omega}) f_M[RL^r(1+a_M R^{\omega/r})], \quad (6)$$

in which a_M and f_M are dependent on the driven process, and b_M is equal to its equilibrium counterpart.

To better elucidate the scaling properties in large-R region, it is convenient to transform the FSS form Eq. (6) into the FTS form. For the driven dynamics starting from the AFM state, we set $RL^r(1+a_M R^{\omega/r}) = c$ (with c a constant), leading to $L = [R(1+a_M R^{\omega/r})/c]^{-1/r}$. Substituting this expression into the leading term of Eq. (6), we obtain

$$M^2(R,L) = [R(1+a_M R^{\omega/r})]^{2\beta/\nu r} \times (1+b_M L^{-\omega}) f_{M1}[RL^r(1+a_M R^{\omega/r})], \quad (7)$$

where the factor $c^{1/r}$ has been absorbed into f_{M1}. In the absence of the scaling correction terms, M^2 recovers its usual FTS form, i.e., $M^2(R,L) = R^{2\beta/\nu r} f_{M1}(RL^r)$.[18–23] From Eq. (7), one finds that for large L and R, the evolution of M^2 from the AFM state should satisfy

$$M^2(R) \propto [R(1+a_M R^{\omega/r})]^{2\beta/\nu r}. \quad (8)$$

Without the finite-R scaling correction term, M^2 follows $M^2(R) \propto R^{2\beta/\nu r}$.[18–23]

In Fig. 4(a), we show results of M^2 starting from the AFM state. It is obvious that even for large L, $M^2(R)$ does not obey $M^2(R) \propto R^{2\beta/\nu r}$, indicating that the scaling corrections should be considered. Upon rescaling R as RL^r, M^2 as $M^2 L^{2\beta/\nu}$ for small R and $M^2 R^{-2\beta/\nu r}$ for large R, one finds that both the small-R and large-R regions exhibit evident deviations in the rescaled curves, as shown in Figs. 4(b) and 4(c),

respectively. Moreover, in the large-R region, the scaling relation $M^2 \propto R^{2\beta/\nu r}$ suggests that the rescaled curves should be parallel to the horizontal axis for large L. However, as seen in Fig. 4(c), the rescaled curves clearly deviate from this expectation, demonstrating that scaling corrections are necessary to fully characterize the behaviors of M^2. In Fig. 4(d), we introduce the finite-size scaling correction to the scaling of M^2, and find that with $b_M = -0.17$ being its equilibrium value,[64] the rescaled curves collapse well in the small-R region, but deviations remain in the large-R region. We further consider the finite-R corrections together according to Eq. (7). In Fig. 4(e), we find that with $a_M = -0.73(1)$, the rescaled curves collapse well across both the small-R and large-R regions, confirming the validity of Eq. (7). In addition, substituting $a_M = -0.73$ into Eq. (8), we find in Fig. 4(a) that with the finite-R correction included, the improved scaling relation Eq. (8) can better describe the behavior of M^2 in the large-R region. As shown in Fig. 4(a), the slope of $M^2(R)$ asymptotically approaches the slope determined by Eq. (8) by as L grows.

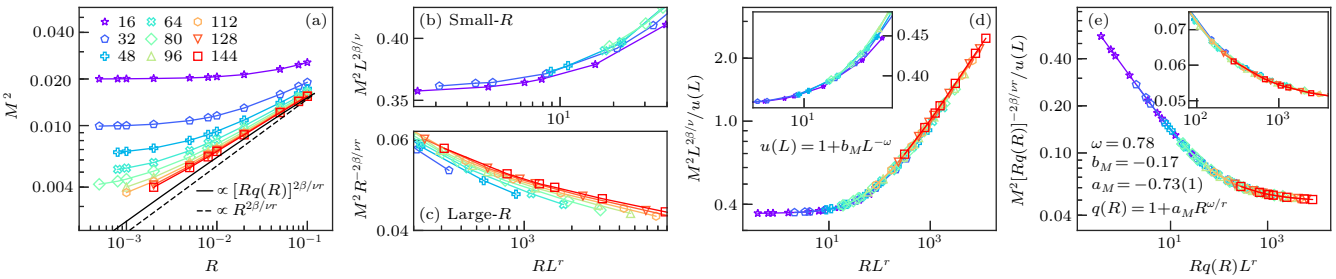


Fig. 4. (a) Dependence of the squared order parameter M^2 on the driving rate R starting from the AFM state with $q_0 = 1$. The solid/dashed line indicates the slope obtained by the scaling relation with/without finite-R corrections. (b) Zoom-in rescaled curves of $M^2 L^{2\beta/\nu}$ versus RL^r for the small-R region. (c) Zoom-in rescaled curves of $M^2 R^{-2\beta/\nu r}$ versus RL^r for the large-R region. Clear deviations in the rescaled curves can be observed in both (b) and (c). (d) Rescaled curves with finite-size correction included. The collapse in the small-R region is significantly improved but deviations still exist in the large-R region as can be seen in the inset. (e) Including both the finite-size and finite-R corrections, the rescaled curves collapse well in the entire scaling region. The flat part of the rescaled curves at large R confirms the validity of the improved scaling relation. The correction power and coefficients are given in panel (e). Log–log scale is applied in all panels.

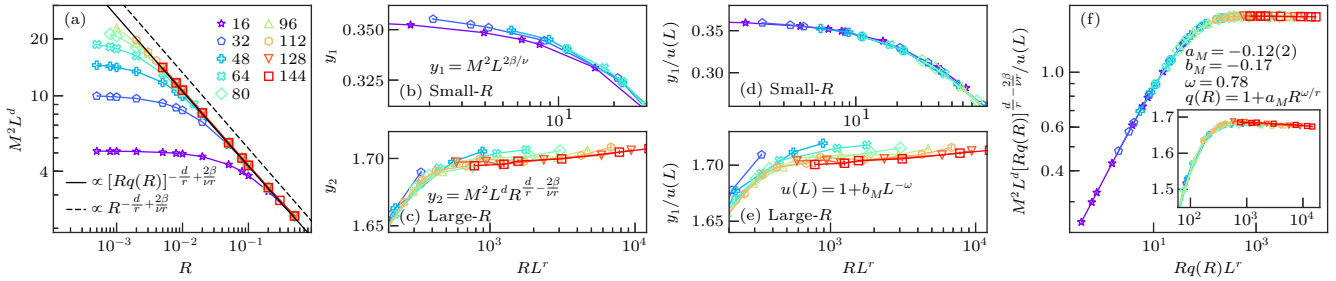


Fig. 5. (a) Dependence of the squared order parameter M^2 on the driving rate R starting from the PM state with $q_0 = 3$. The solid/dashed line indicates the slope obtained by the scaling relation with/without finite-R corrections. The slopes are close, implying that the finite-R correction is not strong for large L and R. (b) Zoom-in rescaled curves of $M^2 L^{2\beta/\nu}$ versus RL^r for the small-R region. (c) Zoom-in rescaled curves of $M^2 L^d R^{d/r - 2\beta/\nu r}$ versus RL^r for the large-R region. Clear deviations in the rescaled curves can be observed in both (b) and (c). (d) and (e) Rescaled curves with finite-size correction included for the small-R and large-R regions, respectively. The collapse in the small-R region is significantly improved but becomes even worse in the large-R region. (f) Including both the finite-size and finite-R corrections, the rescaled curves collapse well in the entire scaling region. The flat part of the rescaled curves at large R verifies the improved scaling relation. The correction power and coefficients are given in panel (e). Log–log scale is applied in all panels.

For the driven dynamics starting from the PM state, the FTS form of M^2 differs from Eq. (7). In this case, M^2 should satisfy

$$M^2(R,L) = L^{-d} R^{2\beta/\nu r - d/r} (1 + a_M R^{\omega/r})^{2\beta/\nu r - d/r} \times (1 + b_M L^{-\omega}) f_{M2}[RL^r (1 + a_M R^{\omega/r})], \quad (9)$$

where the leading term L^{-d} arises from the central limit theorem, which applies when the correlation length is shorter than L.[21,65] Additionally, the coefficient a_M in Eq. (9) is generally different from that for the AFM starting state. For large L, Eq. (9) indicates that, in the large-R region, M^2 should obey

$$M^2(R,L) = L^{-d} R^{2\beta/\nu r - d/r} (1 + a_M R^{\omega/r})^{2\beta/\nu r - d/r}, \quad (10)$$

which restores the usual FTS scaling relation for the PM starting state, i.e., $M^2(R) \propto L^{-d} R^{2\beta/\nu r - d/r}$, when the scaling corrections are neglected.[21,65] In Fig. 5(a) we show the dependence of M^2 on R starting from the PM state. We find that for large L, $M^2(R)$ appears to satisfy $M^2(R) \propto L^{-d} R^{2\beta/\nu r - d/r}$ reasonably well. However, when M^2 is rescaled as $M^2 L^{2\beta/\nu}$ and $M^2 L^2 R^{-2\beta/\nu r + d/r}$, respectively, as shown in Figs. 5(b) and 5(c), significant discrepancies in the rescaled curves arise in both the small-R and large-R regions. Additionally, figure 5(c) shows that rescaled curves of $M^2 L^2 R^{-2\beta/\nu r + d/r}$ versus RL^r are not parallel to the horizontal axis in the large-R region, suggesting that the scaling corrections are necessary. In Figs. 5(d) and 5(e), we introduce the finite-size scaling correction to the

scaling form, and find that only the collapse in the small-R region is significantly improved, leaving the collapse in the large-R region becoming even worse for small L. We further include the finite-R corrections according to Eq. (7), with the coefficient a_M adjustable and $b_M = -0.17$ fixed. From Fig. 5(f), one finds that with $a_M = -0.12(2)$, the rescaled curves collapse very well for all L and R. Note that the value of a_M here is relatively small and rescaled curves are almost flat in the large-R region for large L, these observations imply that the finite-R corrections are not strong for large L and R. This explains why the slopes obtained from the scaling relation with/without finite-R correction look close. Still, we find that with the finite-R correction, the improved scaling relation Eq. (10) with $a_M = -0.12$ describes the behavior of $M^2(R)$ slightly better, as seen in Fig. 5(a).

5. Summary

We have studied the driven critical dynamics in the 2D dimerized Heisenberg model, focusing on the influence of scaling corrections arising from finite driving rate. A modified FTS form, including both finite-size and finite-driving-rate scaling corrections, has been developed. From this scaling form, improved scaling relations have been obtained. We have then verified these full scaling forms and scaling relations for different starting states in the 2D dimerized Heisenberg model using the NEQMC method. Note that the driven dynamic scaling has shown its power in characterizing the quantum phase transitions and preparing various quantum states in fast-developing quantum computers.[32–34] Therefore, it is expected that our present work can be detected in these systems.

Acknowledgments

The authors thank Fan Zhong for helpful discussions. Project supported by the National Natural Science Foundation of China (Grant Nos. 12104109, 12222515, and 12075324), the Science and Technology Projects in Guangzhou (Grant No. 2024A04J2092), and the Science and Technology Projects in Guangdong Province (Grant No. 211193863020).

References

[1] Hohenberg P C and Halperin B I 1977 *Rev. Mod. Phys.* **49** 435
[2] Dziarmaga J 2010 *Advances in Physics* **59** 1063
[3] Polkovnikov A, Sengupta K, Silva A and Vengalattore M 2011 *Rev. Mod. Phys.* **83** 863
[4] D'Alessio L, Kafri Y, Polkovnikov A and Rigol M 2016 *Advances in Physics* **65** 239
[5] Mitra A 2018 *Annual Review of Condensed Matter Physics* **9** 245
[6] Kibble T W B 1976 *J. Phys. A: Math. Gen.* **9** 1387
[7] Zurek W H 1985 *Nature* **317** 505
[8] Laguna P and Zurek W H 1997 *Phys. Rev. Lett.* **78** 2519
[9] Hindmarsh M and Rajantie A 2000 *Phys. Rev. Lett.* **85** 4660
[10] Chuang I, Durrer R, Turok N and Yurke B 1991 *Science* **251** 1336
[11] Dziarmaga J 1998 *Phys. Rev. Lett.* **81** 5485
[12] Zurek W H, Dorner U and Zoller P 2005 *Phys. Rev. Lett.* **95** 105701
[13] Dziarmaga J 2005 *Phys. Rev. Lett.* **95** 245701
[14] Damski B and Zurek W H 2007 *Phys. Rev. Lett.* **99** 130402
[15] Lamporesi G, Donadello S, Serafini S, Dalfovo F and Ferrari G 2013 *Nat. Phys.* **9** 656
[16] Navon N, Gaunt A L, Smith R P and Hadzibabic Z 2015 *Science* **347** 167
[17] Du K, Fang X, Won C, De C, Huang F T, Xu W, You H, Gómez-Ruiz F J, del Campo A and Cheong S W 2023 *Nat. Phys.* **19** 1495
[18] Gong S, Zhong F, Huang X and Fan S 2010 *New J. Phys.* **12** 043036
[19] Zhong F and Xu Z 2005 *Phys. Rev. B* **71** 132402
[20] Zhong F 2011 *Applications of Monte Carlo method in science and engineering*, edited by Mordechai S (IntechOpen, Rijeka)
[21] Huang Y, Yin S, Feng B and Zhong F 2014 *Phys. Rev. B* **90** 134108
[22] Feng B, Yin S and Zhong F 2016 *Phys. Rev. B* **94** 144103
[23] Yin S, Mai P and Zhong F 2014 *Phys. Rev. B* **89** 094108
[24] Zeng Z, Yu Y K, Li Z X, Li Z X and Yin S 2024 arXiv:2403.19258 [cond-mat.str-el]
[25] Zeng Z, Yu Y K, Li Z X and Yin S 2024 arXiv:2408.06138 [cond-mat.str-el]
[26] Wang W, Liu S, Li J, Zhang S X and Yin S 2024 arXiv:2411.06648 [quant-ph]
[27] Deng S, Ortiz G and Viola L 2009 *Europhys. Lett.* **84** 67008
[28] De Grandi C, Polkovnikov A and Sandvik A W 2011 *Phys. Rev. B* **84** 224303
[29] Kolodrubetz M, Clark B K and Huse D A 2012 *Phys. Rev. Lett.* **109** 015701
[30] Chandran A, Erez A, Gubser S S and Sondhi S L 2012 *Phys. Rev. B* **86** 064304
[31] Clark L W, Feng L and Chin C 2016 *Science* **354** 606
[32] Keesling A, Omran A, Levine H, *et al.* 2019 *Nature* **568** 207
[33] Ebadi S, Keesling A, Cain M, *et al.* 2022 *Science* **376** 1209
[34] King A D, Raymond J, Lanting T, *et al.* 2023 *Nature* **617** 61
[35] Sondhi S L, Girvin S M, Carini J P and Shahar D 1997 *Rev. Mod. Phys.* **69** 315
[36] Sandvik A W 2010 *AIP Conference Proceedings* **1297** 135
[37] Chakravarty S, Halperin B I and Nelson D R 1988 *Phys. Rev. Lett.* **60** 1057
[38] Singh R R P, Gelfand M P and Huse D A 1988 *Phys. Rev. Lett.* **61** 2484
[39] Singh R R P 1989 *Phys. Rev. B* **39** 9760
[40] Millis A J and Monien H 1993 *Phys. Rev. Lett.* **70** 2810
[41] Chubukov A V, Sachdev S and Ye J 1994 *Phys. Rev. B* **49** 11919
[42] Troyer M, Kontani H and Ueda K 1996 *Phys. Rev. Lett.* **76** 3822
[43] Kim J K and Troyer M 1998 *Phys. Rev. Lett.* **80** 2705
[44] Matsumoto M, Yasuda C, Todo S and Takayama H 2001 *Phys. Rev. B* **65** 014407
[45] Wang L, Beach K S D and Sandvik A W 2006 *Phys. Rev. B* **73** 014431
[46] Giamarchi T, Ruegg C and Tchernyshyov O 2008 *Nat. Phys.* **4** 198
[47] Sachdev S 2008 *Nat. Phys.* **4** 173
[48] Merchant P, Normand B, Kramer K W, Boehm M, McMorrow D F and Ruegg C 2014 *Nat. Phys* **10** 373
[49] Lohöfer M, Coletta T, Joshi D G, Assaad F F, Vojta M, Wessel S and Mila F 2015 *Phys. Rev. B* **92** 245137
[50] Wenzel S, Bogacz L and Janke W 2008 *Phys. Rev. Lett.* **101** 127202
[51] Qin Y Q, Normand B, Sandvik A W and Meng Z Y 2015 *Phys. Rev. B* **92** 214401
[52] Ma N, Weinberg P, Shao H, Guo W, Yao D X and Sandvik A W 2018 *Phys. Rev. Lett.* **121** 117202
[53] Wu J, Yang W, Wu C and Si Q 2018 *Phys. Rev. B* **97** 224405
[54] Tan D R, Li C D and Jiang F J 2018 *Phys. Rev. B* **97** 094405
[55] Tan D R and Jiang F J 2020 *Phys. Rev. B* **101** 054420
[56] Sandvik A W and Scalapino D J 1994 *Phys. Rev. Lett.* **72** 2777
[57] Rønnow H M, McMorrow D F, Coldea R, Harrison A, Youngson I D, Perring T G, Aeppli G, Syljuåsen O, Lefmann K and Rischel C 2001 *Phys. Rev. Lett.* **87** 037202
[58] Manousakis E 1991 *Rev. Mod. Phys.* **63** 1
[59] Löhneysen H v, Rosch A, Vojta M and Wölfle P 2007 *Rev. Mod. Phys.* **79** 1015
[60] Shu Y R, Jian S K, Sandvik A W and Yin S 2025 *Nat. Commun.* **16** 3402
[61] De Grandi C, Polkovnikov A and Sandvik A W 2013 *J. Phys.: Condens. Matter* **25** 404216
[62] Liu C W, Polkovnikov A and Sandvik A W 2013 *Phys. Rev. B* **87** 174302
[63] Guida R and Zinn-Justin J 1998 *J. Phys. A: Math. Gen.* **31** 8103
[64] Cai J Q, Shu Y R, Rao X Q and Yin S 2024 *Phys. Rev. B* **109** 184303
[65] Liu C W, Polkovnikov A and Sandvik A W 2014 *Phys. Rev. B* **89** 054307